The Holocene 9,6 (1999) pp. 659–669

Calibration of the speleothem delta function: an absolute temperature record for the Holocene in northern Norway

Stein-Erik Lauritzen[1] and Joyce Lundberg[2]

([1]Department of Geology, Bergen University, Allégaten 41, N-5007 Bergen, Norway; [2]Department of Geography, Carleton University, Ottawa, Ontario K1S 5B6, Canada)

A HOLOCENE SPECIAL ISSUE

Abstract: The speleothem delta function (SDF) provides a new transfer function between the $\delta^{18}O$ signal of speleothem calcite and surface ground temperature. The function is based on physical principles, relating $\delta^{18}O$ of the calcite to thermodynamic fractionation, and to the *dripwater function*, which in turn relates $\delta^{18}O$ of dripwaters to that of the local precipitation and thus to the modification of source water in relationship to the geographical position of the site. The SDF must be calibrated against at least two reliable and well-dated palaeotemperature points. The end product is a reconstruction of absolute cave and surface temperatures. The technique is tested using a Holocene speleothem from north Norway, SG93, dated by 12 TIMS U-Th dates. The reconstructed temperature curve is presented and compared with the GISP2 ice-core record and with the historic record. In both cases the correlation with SG93 is impressive, indicating the validity of the technique.

Key words: Speleothem, palaeoclimate, proxy, transfer function, oxygen isotopes, ^{18}O, speleothem delta function, uranium-thorium dating, Holocene, Norway.

Introduction

Speleothems (cave dripstones) offer a unique data source for continental climatic proxy signals, such as stable isotopes (Schwarcz, 1986; Gascoyne, 1992), annual growth laminae (Baker *et al.*, 1993; Shopov *et al.*, 1994), pollen (Bastin, 1978; Lauritzen *et al.*, 1990) and organic matter (Lauritzen *et al.*, 1986; Ramseyer *et al.*, 1997). Moreover, these proxy records can be precisely dated by U-series techniques, yielding a timescale in calendar years (Latham and Schwarcz, 1992). Using thermal ionization mass spectrometry (TIMS) to measure the uranium-series disequilibria can produce dates of extreme precision (Chen *et al.*, 1992). Given that suitable material is available, TIMS dating is superior to conventional AMS ^{14}C dates, not only with respect to analytical precision, but also because no conversion between ^{14}C years and calendar years is necessary for U-series dates. At present the dating limit with U-Th techniques is almost 750 000 years; thus speleothem records cover much more time than most other terrestrial archives.

The stable isotope composition of speleothem calcite reflects both rainwater isotopic composition ($\delta^{18}O$) and soil productivity ($\delta^{13}C$) (Gascoyne, 1992). Since the aim of most palaeoclimatic studies is to produce physical parameters that can be tested against climate models, it is of paramount interest to separate out a pure temperature signal from the records. The challenge of using stable isotopes in speleothem for palaeoclimatic research is to find a unique functionality between temperature and the $\delta^{18}O$ signal that is based on physical principles rather than empiricism. Here, we attempt to do this and present a calibration of the local temperature response of a speleothem and transform it into a high-resolution temperature time-series for the Holocene of north Norway.

Oxygen isotopes: the speleothem delta function (SDF)

Provided that the calcite is precipitated in isotopic equilibrium with the dripwater, according to the Hendy criteria (Hendy, 1971; Gascoyne, 1992), the oxygen-isotope composition of the calcite ($\delta^{18}O_c$) is a function of the isotopic composition of the dripwater ($\delta^{18}O_w$) (Fritz and Fontes, 1980):

$$\alpha_{c\text{-}w} = \frac{\delta^{18}O_c + 1000}{\delta^{18}O_w + 1000} \tag{1}$$

where $\alpha_{c\text{-}w}$ is the temperature-dependent fractionation constant between calcite and water (O'Neil *et al.*, 1969). This can also be expressed as:

$$\alpha_{c\text{-}w} = e^{\left(\frac{a}{T} - b\right)} \tag{2}$$

where T is temperature in Kelvin and the two constants, a and b, govern the fractionation factor between the carbonate mineral and water ($\alpha_{c\text{-}w}$) (Friedman and O'Neil, 1977).

The two equations may be combined (Dorale *et al.*, 1992),

 0959-6836(99)HL351RP

solved with respect to $\delta^{18}O_c$, and modified to give a new expression: the *speleothem delta function* (SDF) (Lauritzen, 1995; 1996):

$$\delta^{18}O_c = e^{\left[\frac{a}{(T_1+273.15)} - b\right]} [F(T_2, t, g) + 10^3] - 10^3 \qquad (3)$$

where T_1 is the cave temperature and T_2 is the surface temperature representative for the precipitation, both in degrees Centigrade, t is time and g is the geographical position of the site. Normally, due to ventilation effects, the deep cave temperature approaches the annual mean air temperature at the surface (Wigley and Brown, 1976), so that T_1 can be assumed equal to T_2. The SDF (equation 3) has two terms: the first (exponential) term represents the thermodynamic fractionation (*TFr*) between calcite and water, and the second term contains the *dripwater function*, $F(T_2, t, g)$. Here, the T-dependence (T_2) relates to the atmospheric precipitation at a site, while the t- and g-dependence represent the transport history of rain and various properties of the climate system producing the rainfall and source water variations. This (t- and g-) sensitivity is further controlled by storage and mixing of the percolation water above the cave. The simplest representation of the storage/mixing effect is an average:

$$\delta^{18}O_w = \frac{1}{\theta} \sum_{n=1}^{\theta} [\delta^{18}O_p]_n \qquad (4)$$

where θ is the time of averaging, and the indexes 'w' and 'p' represent dripwater and atmospheric precipitation respectively. Such an approach may be over-simplistic; for instance, there might be a seasonal interception bias in aquifer recharge above the cave, dependent on the fraction of precipitation that actually enters the epikarst (Lauritzen, 1995).

Assuming that there is a simple relationship between $\delta^{18}O_w$ and $\delta^{18}O_p$ as in equation (4), then the simplest way to model F(T, t, g) may be to use a modified Dansgaard (1964) equation:

$$F(T, t, g) \approx \delta^{18}O_p = cT + d + \Delta_{SMOW}(t) \qquad (5)$$

where c and d are adjustable parameters. The equation expresses the isotopic composition of the dripwater relative to mean ocean seawater. Normally, $\Delta_{SMOW}(t)_{t=0}$ is by definition zero and not a part of equation (5). However, because seawater composition would change back in time due to the ice-volume effect, $\Delta_{SMOW}(t)$ must be taken into account. Note that equation (5) is simplistic in the sense that the parameters c and d are assumed to be constant over the time-range in question. However, it is already known that c and d are dependent on the present-day climatic system, i.e., the geographic position (Dansgaard, 1964), so that they would certainly change over time if climate changed considerably. Since equation (3) and equation (5) are expressed in vPDB and vSMOW units respectively, unit conversion has to be performed on equation (5) before substitution in equation (3).

The components *TFr* and F(T, t, g) have different temperature sensitivities. *TFr* always has a negative response to temperature (i.e., heavier $\delta^{18}O_c$ values imply decreasing temperature), while F(T, t, g) may respond either positively or negatively, depending on regional meteorology. Consequently, the temperature response of speleothem carbonate is entirely dependent on the relative magnitude of *TFr* and F(T, t, g). The *temperature response rate* (μ) of equation (3) is, in mathematical terms, its T-derivative (Lauritzen, 1995) defined as:

$$\mu = \frac{\partial}{\partial T} (\delta^{18}O_c) \qquad (6)$$

which can, in principle, be negative, zero or positive. This can be further elucidated with respect to the relative magnitudes of T-responses of (*TFr*) and of F(T, t, g) (Table 1).

TFr alone will give $\mu < 0$ but in the cases of $\mu > 0$ or $\mu \ll 0$ variations in $\delta^{18}O_w$ of the precipitation dominate. The temperature sensitivity and therefore the interpretation of speleothem $\delta^{18}O_c$ is by no means straightforward and often ambiguous, but the problem may be overcome in ways that either aim at estimating F(T, t, g), or just estimating the *sign* of μ:

- First, F(T, t, g) at a given point in time and space can be estimated from fluid inclusions within the calcite, which are actual samples of the original dripwater at the time of precipitation. Due to post-depositional exchange with the surrounding calcite, $\delta^{18}O_w$ = F(T, t, g) cannot be measured directly in the water, but must be estimated from δ^2H_w, via the so-called 'meteoric water line', or a local equivalent (Craig, 1961; Gat, 1980):

$$\delta^{18}O_w = \frac{1}{8}\,\delta^2H_w - \frac{10}{8} \qquad (7)$$

  Then, temperature can be calculated directly from the thermodynamic term of equation (1) (Schwarcz and Yonge, 1983; Rowe *et al.*, 1998).
- Second, independent evaluation of palaeowater $\delta^{18}O_w$ may be extracted from other sources, such as fossil aquifers (Talma and Vogel, 1992).
- Third, by comparing trends in the $\delta^{18}O_c$ time-series with present-day $\delta^{18}O_c$ of stalactite tips (i.e., Holocene, non-glacial conditions) and known climatic changes in the past, the sign of (μ) may be judged and assumed valid for the rest of the time-series (Schwarcz, 1986).
- Finally, given that some independent temperature estimates exist for both present and past conditions, the constants c and d in the combined equations (3) and (5) may, in principle, be determined. Assuming that the values of the two constants are valid for timespans beyond the calibration range, the $\delta^{18}O_c$ record may then be transformed to absolute temperature (Lauritzen, 1996; Lauritzen and Lundberg, 1998).

When applying the latter technique, at least two data points in the temperature-time space are needed. One such point ($\delta^{18}O_c$,T) is immediately available: present-day conditions represented by the annual mean surface temperature (as measured instrumentally inside the cave) and $\delta^{18}O_c$ of recent calcite. If the stalagmite was still growing when collected, the most representative sample of recent calcite would be its top surface. If the speleothem for some reason was relict, the tips of actively growing stalactites in close proximity to the sample must be used.

Table 1 Temperature response of the speleothem delta function

		Overall response	Dripwater function
1:	$\mu > 0$	$\delta^{18}O_c$ gets heavier with increasing temperature	F(T, t, g) response is positive and large enough to dominate over *TFr*
2:	$\mu = 0$	$\delta^{18}O_c$ does not change with temperature	*TFr* and F(T, t, g) responses cancel each other
3:	$\mu < 0$	$\delta^{18}O_c$ gets lighter with increasing temperature	*TFr* is dominant and/or F(T, t, g) response is negative or weakly positive

Other points in the temperature-time space must be found for some well-defined climatic events that can be clearly identified in the sample and for which independent temperature estimates exist. Since the calibration procedure involves curve fitting by regression, the precision of the transfer function depends upon the number of calibration points, their fit to the function and on the precision of each individual calibration point. The application of this technique is explained below using as a case study a speleothem from north Norway.

Material and methods

Sample site

The speleothem sample SG93 was collected in the summer of 1993 from the deepest sections of Søylegrotta, Mo i Rana, northern Norway (Figure 1). The cave entrances are situated at 280 m a.s.l. in a small depression in the side of Dunderlandsdalen some 10 km east of Mo i Rana. The cave, which is essentially relict, is developed in calcite marble at the contact zone against ferruginous mica schists (Figure 2). The only available natural entrance was through a streamsink shaft, but a second entrance was opened by digging in the late 1960s. Since then, some parts of the cave have displayed weak seasonal draughts. The cave is well decorated with speleothems, of which the oldest U-series (TIMS) date is almost 700 ka. The sample grew on a bank of stream gravel in the deepest and most remote part of the cave, approximately 100 m below the surface.

Cave microclimate

The cave microclimate was monitored with an Aanderaa Instruments® data logger system (1991–1993) in order to determine, at 1 h intervals, drip rates, air pressure, temperature, etc. Due to logistic constraints and power failures, it was not possible to acquire a continuous record all through the period of measurement, but a composite one-year cycle, representing the years 1991 and 1992, is shown in Figure 3a (Einevoll and Lauritzen, 1994). The cave temperature is, as expected, very stable and approaches the mean annual air temperature on the surface. The cave air temperature is +2.8 ± 0.32°C. The mean annual temperature for a nearby meteorological station (Neverdal, 36 m a.s.l.; 1966–1989) is +3.6 ± 1.0°C (DNMI, 1998). Correction for the adiabatic lapse rate (0.6°C/100 m) over the 150 m altitude difference between the cave site and the climate station yields a mean annual surface temperature of 2.7 ± 1.0°C, i.e., very close to the measured deep cave temperature. This strongly suggests that the theory of Wigley and Brown (1976) holds true for this cave site.

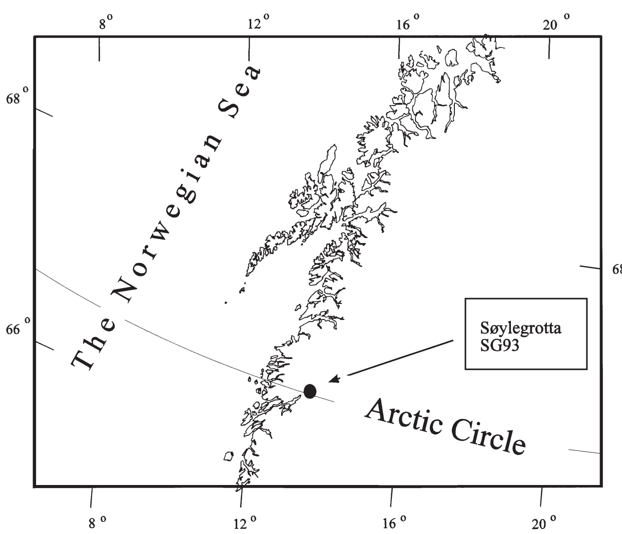

Figure 1 Location of Søylegrotta in northern Norway.

Dripwater and recent calcite

At 10 different stations, stalactite dripwater was collected regularly over two years and analysed for oxygen isotopes. Also, samples of atmospheric precipitation were taken at irregular intervals at a nearby farm. As expected, the cave dripwaters display almost constant isotopic composition, due to storage and mixing in the unsaturated zone, while the atmospheric precipitation varied by almost 20‰ (Figure 3b). At the end of the observation period, the respective stalactite tips were collected and analysed. From these pairs of $\delta^{18}O_c$ and $\delta^{18}O_w$, the corresponding temperatures were calculated (equations 1 and 2), assuming isotopic equilibrium conditions during crystal growth. The isotopic temperature is 2.74 ± 1.13°C for three stalactites close to SG93, where draughts were negligible. Hence, the recent calcite precipitated next to SG93 reflects the cave air temperature as well as the surface annual mean temperature quite well.

Sample description

The stalagmite sample SG93 was 32 cm tall and about 8 cm wide at the base. The sample was split open into two parallel wafers along its central axis, leaving two lateral pieces.

In section (Figure 4) the sample consisted of white, translucent calcite, displaying occasional white growth bands rich in fluid inclusions. Large calcite crystallites could be traced from the growth axis radially out through the growth surfaces. At 147 mm, the cave was probably flooded, because a dirty layer, in part brown-coloured due to humics (Lauritzen *et al.*, 1986), was draped over the growing speleothem. At about 270 mm from the base, the growth axis shifted sideways and continued at about 60° until growth was halted. The top surface, no longer active at the time of collection, displayed re-solution phenomena in the form of small cavities and irregular fabric. The base of the stalagmite encrusted mica schist and marble gravels.

Analysis

One wafer was polished, photographed and used for the stable isotope traverse. Samples of 0.2 mg calcite were extracted with a dental drill at 1 mm intervals along the whole sequence, yielding 328 separate positions. Stable isotopes of carbon and oxygen were measured by CO_2 expulsion with H_3PO_4 and analysed on a Finnigan 251 instrument at the Geological Mass Spectrometry lab in Bergen.

Twelve subsamples for TIMS U-series dating (0.6–1.7 g) were sectioned by means of a dentist's cutting disk from a 20 × 8 mm thick rod that was cut along the central growth axis on one of the wafers. The subsamples were ignited in quartz crucibles at 800°C for 4–6 hours in order to destroy organics and expel CO_2. The resulting CaO was dissolved in H_2O/HNO_3, a Fe carrier and spike added (JL369, DIL-E; $^{229}Th : ^{233}U : ^{236}U \sim 0.2 : 0.5 : 1.0$). Spiking levels were aimed at an atomic ratio between $^{234}U_{sample}$ and $^{233}U_{spike}$ of 0.5–1. The radionuclides were scavenged on $Fe(OH)_3$, cleaned by anion exchange chromatography in 7.5 M HNO_3, and separated with 6 M HCl and 1 M HBr. This process was repeated once. The purified U and Th fractions were evaporated to dryness and taken up in 0.1 M H_3PO_4. All chemical preparations were performed in an overpressured cleanlab with laminar flow hoods, using either Suprapur® (Merck) or doubly (sub-boiling) distilled reagents. Both U and Th were loaded onto single Rhenium (5 × zone-refined) filaments. Typically, all of the Th fraction, and an amount of U corresponding to ~100 ng ^{238}U, was loaded. U was run as oxide from a silica gel bed, while Th was run as metal from a graphite sandwich. Mass abundancies of ^{236}U, ^{235}U, ^{234}U, ^{233}U, ^{229}Th, ^{230}Th, and ^{232}Th were measured on a Finnigan 262 RPQ instrument in dynamic (ion counting) mode. Data reduction,

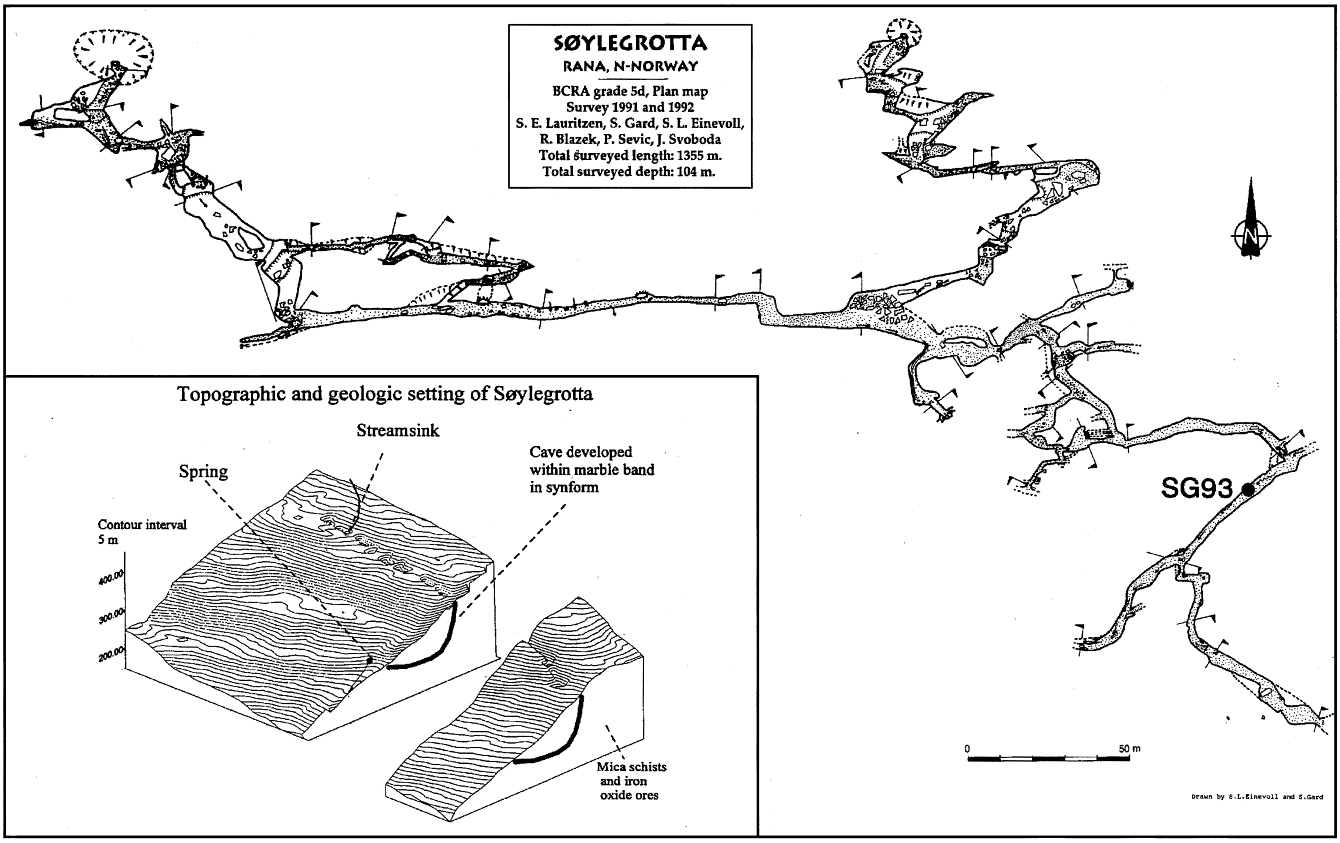

Figure 2 Survey of Søylegrotta, with sample location (SG93). Inset: terrain position and geological situation. The cave is developed within a relatively thin marble band, so that the two entrance sections consists of steeply inclined passages and shafts. The lowest parts of the cave are largely horizontal and end in sumps and sediment chokes. The vertical percolation path for speleothem feedwater is almost 100 m through mica schists and marble bands.

error optimization and propagation were done on tailored software (Lauritzen and Lundberg, 1997a; 1997b).

Results and discussion

U-series dating

The U-series dating results are shown in Table 2. All errors are $\pm 2\sigma$; the average error over the 10 kyrs is 22 years. Decreasing $^{230}Th/^{232}Th$ ratio in young samples (e.g., after *c.* 5 ka) is basically a function of age and does not necessarily indicate detrital content. In this case, all $^{234}U/^{232}Th$ values are high indicating low ^{232}Th levels. We have therefore decided not to perform any correction for presumed non-authigenic ^{230}Th, simply because there is no convincing evidence that age is affected by absolute ^{232}Th concentration. Second, the 'raw' ages display a very regular stratigraphic order along the sequence. Third, the correction factor of initial, non-authigenic ^{230}Th ($[^{230}Th/^{232}Th]_0 = 1.5$; see Schwarcz, 1980), commonly used in α-particle dating, is an *average* value for detrital environments, and thus quite arbitrary for a northern Norwegian speleothem.

The time model

The relationship between age and sampling position is shown in Figure 5: individual ages for the time-series were interpolated using a parabolic function for most of the sample, and a linear function for the top 1000 years. This results in an average error in the *interpolated* age of ± 46 years for the period (0–9 ka) and ± 174 years for ages around 9 ka. However, growth was very slow at the base (beyond 9 ka) so that a lot of time is integrated in each sample. Hence, in spite of each TIMS *analysis* being very precise, the age is only an *average* over a long timespan, so that the extreme basal ages of the sequence could easily have an error of 1000 years or more. Because of this, the isotopic rise at the base of the sequence (*vide infra*) does not contradict the post-Preboreal warming observed in other records, such as the Greenland ice cores around 10 500 calendar years BP (Alley *et al.*, 1997).

Hendy criteria

As mentioned, due to the TFr term (equation 3), the SDF can only be applied provided that the speleothem calcite crystallized in isotopic equilibrium with the dripwater, i.e., that there was no significant bias from kinetic fractionation in the oxygen isotopes between the water and the solid $CaCO_3$ phase. The Hendy criteria (1971; Schwarcz, 1986) for testing if calcite was precipitated in isotopic equilibrium require that there be neither correlation between $\delta^{18}O$ and $\delta^{13}C$ of *successive samples* taken along the same growth layer, nor any significant changes in $\delta^{18}O$ *along the same growth layer* when traversed across the apex and down the side of the sample. The theory is that, if *kinetic fractionation* (i.e., non-isotopic equilibrium) occurred during precipitation, $\delta^{18}O$ and $\delta^{13}C$ would both change in concert as the water film ran off the sides of the stalagmite. If precipitation occurred under *isotopic equilibrium*, $\delta^{18}O$ would remain constant, while $\delta^{13}C$ would change progressively along the traversed path.

This was tested for two traverses (at 37 mm and 252 mm; Figure 6). Following Gascoyne (1992), the maximum tolerance in $\Delta\delta^{18}O_c$ along a single growth layer is set to 0.8‰. In neither of the two traverses is there any significant correlation between $\delta^{18}O$ and $\delta^{13}C$, nor is there any significant variation in $\delta^{18}O$ down the sides of the sample. We may therefore conclude that the speleothem grew in isotopic equilibrium with the parent dripwater.

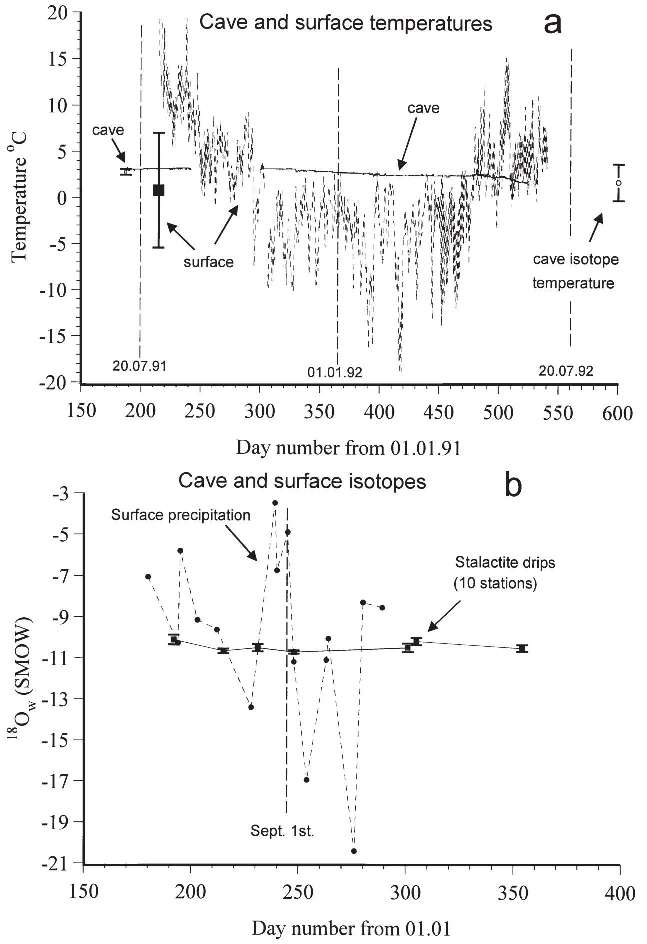

Figure 3 Cave microclimate and stable isotopes. (a) Composite one-year cycle (1991–1992) of cave and surface temperatures: dashed curve, surface air temperature above cave; solid curve, cave temperature. The cave temperature is almost constant, and mimics the surface annual mean. The ambient cave temperature, calculated from the oxygen isotope composition of 10 stalactite dripwater samples through one year (see Figure 3b) and calcite from the tips of the same samples, also corresponds with the annual mean (see text for further discussion). (b) Isotopic composition of atmospheric precipitation (dashed line and black dots), plotted with the mean isotopic composition of 10 stalactites in the cave during 1991.

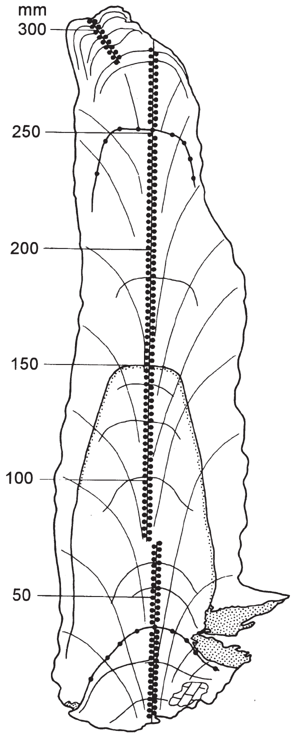

Figure 4 Sample SG93, with sampling positions for stable isotopes (black dots). Note the two growth bands: traverse 1 (at 35 mm) and traverse 2 (at 252 mm). The dirty growth band at 150 mm is also shown. Dotted areas are sand and silt inclusions.

Calibration of the SDF

Calibration of the SDF requires a set of reliable, independent temperature estimates at given points in time, which can be matched to corresponding isotopic values of the cave calcite. This is not straightforward and involves various correlation problems. First, most Holocene temperature estimates are based on biological indices (pollen, tree-lines, diatoms) or glaciological evidence: they all describe variations in growth/ ablation season temperatures, which is either summer mean or July temperatures. According to the theory of cave ventilation (Wigley and Brown, 1976) and supported by direct measurements, the cave temperature can be assumed to approach the annual mean surface temperature. Moreover, the temperature term in the SDF represents a combination of average surface temperature representative for the precipitation and the cave temperature at the stalagmite. Hence there is a potential problem in matching shifts in *mean summer* temperatures with shifts in *mean annual* temperatures. Second, these temperature estimates are rarely derived in sites that are completely equivalent to the cave site, so that data from similar sites must be preferred, and assumptions of *validity* must be allowed for. Third, the timing of these temperature events are much less precise than the speleothem record and they also display large temporal variation. Thus there is a problem of knowing whether the biological record has picked up an extreme (threshold-dependent) event, or represents

Table 2 TIMS Uranium series dates of sample SG93

Subsample	mm from base	U (ppm)	$^{234}U/^{238}U$	$^{230}Th/^{234}U$	$^{230}Th/^{232}Th$	Age, kyr $\pm 2\sigma$
157-1A	–5–0	0.968 ± 0.0007	1.7412 ± 0.00305	0.09185 ± 0.0002	21.0 ± 0.7	10.409 ± 0.021
042-3B	0–3	0.976 ± 0.0011	1.6855 ± 0.00404	0.08788 ± 0.0002	36.0 ± 1.5	9.944 ± 0.022
158-4/6	4–6	0.911 ± 0.0006	1.6916 ± 0.00264	0.08400 ± 0.0002	37.0 ± 0.8	9.488 ± 0.019
043-14M	22–24	0.963 ± 0.0005	1.6472 ± 0.00222	0.07269 ± 0.0002	58.0 ± 1.6	8.169 ± 0.024
044-4C	45–47	1.480 ± 0.0007	1.6280 ± 0.00184	0.06471 ± 0.0001	192.0 ± 0.6	7.246 ± 0.017
045-5D	48–50	1.545 ± 0.0006	1.6549 ± 0.00162	0.06265 ± 0.0001	158.0 ± 0.6	7.008 ± 0.016
046-7F	100–102	1.242 ± 0.0006	1.6706 ± 0.00176	0.04585 ± 0.0001	79.0 ± 1.0	5.090 ± 0.016
047-10I	143–145	1.410 ± 0.0016	1.5544 ± 0.00391	0.03527 ± 0.0001	76.0 ± 1.0	3.897 ± 0.011
048-8G	148–150	1.420 ± 0.0013	1.6611 ± 0.00404	0.03244 ± 0.0001	48.0 ± 0.7	3.579 ± 0.009
049-12K	200–202	1.270 ± 0.0007	1.6657 ± 0.00201	0.01943 ± 0.0003	69.0 ± 1.6	2.131 ± 0.031
050-AC3	250–257	2.100 ± 0.0022	1.6570 ± 0.00376	0.00964 ± 0.0001	44.0 ± 1.2	1.053 ± 0.007
051-AB2	300–305	1.150 ± 0.0005	1.6856 ± 0.00170	0.00232 ± 0.00002	4.0 ± 1.3	0.253 ± 0.002

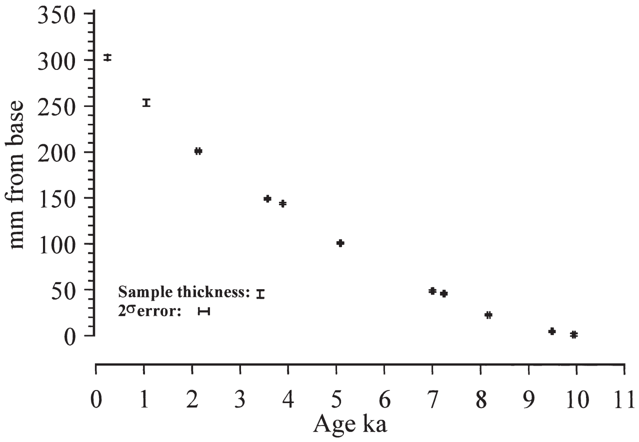

Figure 5 Age and sample positions for SG93. The actual age estimates were done by interpolation of a parabolic growth model for ages >1000 years, and by a linear growth model for ages <1000 years. Age errors were propagated from radiometric errors and sampling intervals.

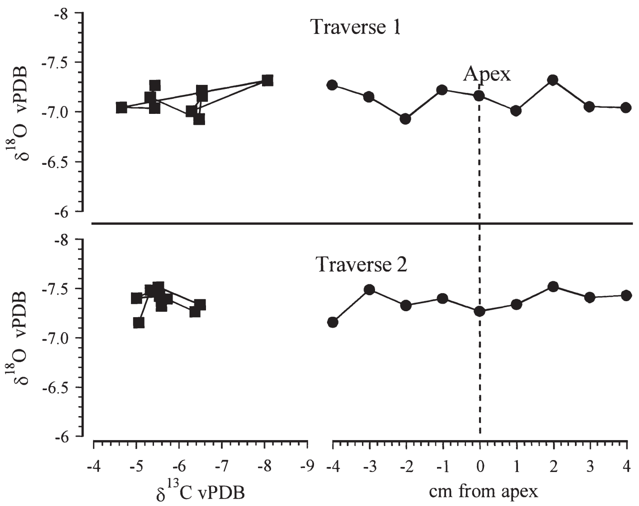

Figure 6 Hendy test for the two growth bands at 37 and 252 mm of SG93 (see Figure 4).

an average over some timespan, and in turn, how a representative isotope value can be matched to it. Here, we have chosen to approach the calibration problem by first using the 'Little Ice Age' (LIA) temperature drop, which is well defined both with respect to time and temperature, and then *testing* whether this calibration is meaningful in the context of other temperature estimates. This is done because we regard the LIA temperature drop as the most reliable of those temperature estimates that are presently available for calibration of the SDF (*vide infra*).

Correction for Δ_{SMOW}

Because seawater composition would change back in time due to the ice-volume effect, $\Delta_{SMOW}(t)$ – from a theoretical point of view – must be taken into account, as in equation (5). The ice-volume effect is generally regarded as 1.2–1.8‰ between glacial and interglacial conditions (Shackleton and Opdyke, 1973). This was modelled by using the global deep-sea isotopic curve of Martinson *et al*. (1987), expressed as $\Delta_{SMOW}(t) = SMOW_0 – SMOW(t)$, i.e., the change in ocean composition between the present value, $SMOW_0$, and at some given point in time. $\delta_{SMOW}(t)$ was then substituted in equations (5) and (3) and solved for T. The resulting temperature shift from the Δ_{SMOW} correction can then be assayed by calculating T at a given time with and without the $\Delta_{SMOW}(t)$ term. The magnitude of this correction is proportional to the ice-volume effect and is thus neglible for ages less than a few thousand years. At 10000 calendar years BP, it amounts to ~1°C.

Independent temperature information

A vast range of palaeotemperature proxy data for various parts of the Holocene are available, but only a few may be characterized as sufficiently precise in timing and absolute temperature estimates to be used for calibration of the SDF. The following data sets are well defined and therefore taken as possible calibration points for SDF. They are also derived from sites that are reasonably near the site of SG93. The data are summarized in Table 3, where the temperature difference between today and the respective events have been transformed to corresponding temperatures at the cave site, and the magnitude of the Δ_{SMOW} correction on temperature estimated and subtracted to yield a 'corrected' temperature for use in the SDF calibration and testing.

(i) *Present-day conditions*. The mean annual air temperature for Mo I Rana of + 2.7°C represents the isotope values of stalactite tips in the close vicinity of sample SG93 (–7.33‰ vPDB). As mentioned above, the cave temperature and the isotope tempera-

Table 3 Calibration data for the speleothem delta function

Event/condition	Age[a]	Δ_{SMOW} temp[b]	Local temp[c]	Temp diff[d]	Temp[e]	Corr temp[f]	$\delta^{18}O_c$	Ref
'Permafrost' (percolation threshold)	<9500	1			>–1	–2	–6.24	1
Cave temperature	0	0		0	2.8	2.8	–7.44	2
'Little Ice Age'	200	0		1.0	1.8	1.8	–7.12	3
Tree-line drop	3700	0		–1.5	1.3	1.3	–6.6	4
Diatoms	≈7000 (7590–5900)	0.4	11.5	+1.7	4.10	4.1	–7.9	5

All temperatures are in °C, $\delta^{18}O_c$ in ‰ vPDB.
[a]Cal BP, approximate age of evvents.
[b]Temperature shift if SMOW correction is applied.
[c]Absolute temperature estimate at site.
[d]Difference between present-day and respective temperature event.
[e]Temperature converted to the cave site.
[f]Temperature at cave site corrected for SMOW.
References: (1) French (1976); (2) Data logger measurements in cave; (3) Nesje and Kvamme (1991); (4) Lake diatoms, Abisko, Swedish Lapland, Hall *et al*. (1998); (5) Barnekow and Berglund (1988).

ture calculated from stalactite tips and dripwater correspond quite well to the annual mean air temperature of the site, which is taken as supporting evidence for this assumption. $\Delta_{SMOW}(0)$ is by definition zero and need not be corrected for.

(ii) *The 'Little Ice Age' (LIA)*. The sample was not actively growing when collected. Since TIMS dating gave an average age of 253 years for the top 5 mm with a 'cooling' trend in the isotopes (Figure 7), the coldest signal (–7.12‰) here is taken as an extreme LIA signal. Depression of the Equilibrium Line Altitude (ELA) measured from terminal and lateral moraines corresponds to a temperature drop of about 1°C during the LIA (Nesje and Kvamme, 1991). Δ_{SMOW} is insignificant and is not corrected for.

(iii) *Tree-line changes*. Lake sediment sequences with pollen and plant macrofossils in the Abisko area of northern Sweden have revealed a distinct drop in pine and mountain birch tree limits at about 3700 cal. BP, corresponding to a growth season temperature drop of around 1.5°C (Barnekow and Berglund, 1998). The corresponding average isotopic composition in SG93 for this time interval is about –6.6‰ vPDB. Δ_{SMOW} is also insignificant at this time.

(iv) *Diatoms in lake sediments*. Analyses of diatom communities in lake sediments from the Sarek Mountains, northern Sweden, indicate July temperatures up to 1.7°C higher than today during the period 7590–5900 cal. BP (Hall *et al.*, 1998). The corresponding average isotopic composition in SG93 for this time interval is about –7.9‰ vPDB. Δ_{SMOW} correction for this time interval corresponds to –0.4°C.

(v) *Commencement of speleothem growth after permafrost conditions*. This is the least reliable calibration point. Generally, if a speleothem is already established, permafrost conditions will halt growth and the layer of calcite immediately above the hiatus will therefore be indicative of release from permafrost conditions. However, SG93 was not already established before the onset of permafrost conditions; we do not know if there was any delay between ground melting and establishment of this route for dripwater. Growth of SG93 did not commence until some time before 10 500 cal. BP but was very sluggish so that the exact timing is difficult to determine. However, within the supposed age error at the extreme base of SG93, the growth commencement coincides roughly with the Younger Dryas/Boreal transition (11 500 cal. BP) and was probably controlled by both CO_2 supply and liquid water. It is reasonable to assume that the 'coldest' isotopic values recorded in the calcite at this time may correspond to surface temperatures slightly higher than those that would support permafrost. In general, permafrost is supported in areas having annual mean air temperatures lower than –1°C (Price, 1972; French, 1976). However, if there was a delay in the establishment of the drip route, then the coldest isotopic values in the speleothem will represent a temperature more than only 'slightly higher' than this. Since the Δ_{SMOW} correction at 9–10 ka amounts to a temperature increase of ~1°C (*vide infra* in Figure 9), this has to be taken into account in the calibration. The corrected temperature at the 'coldest' observed isotope value (–6.20‰ vPDB) is therefore set to –2.0°C (Table 3).

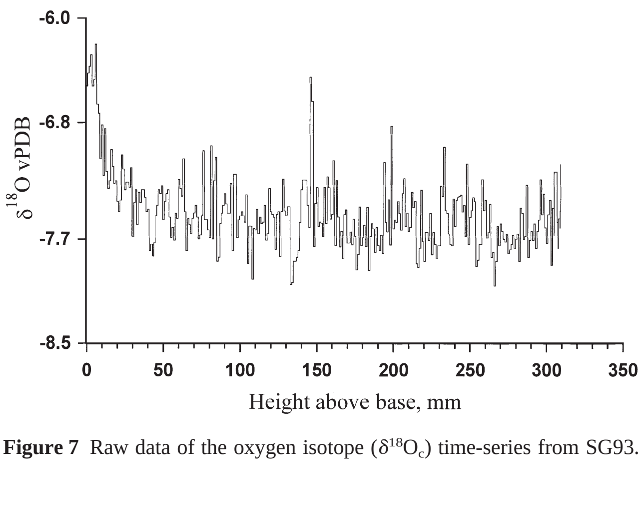

Figure 7 Raw data of the oxygen isotope ($\delta^{18}O_c$) time-series from SG93.

Calibration against the LIA temperature drop

The SDF was first calibrated using only the present temperature and that of the LIA. When seen in combination, the non-zero top age of the sample (about 200 years), the anomalous morphology at the tip (re-solution hiatus), and the progressive cooling displayed by the $\delta^{18}O_c$ signal (increases to heavier values than the present), suggest that growth was halted during a cold spell within the LIA. Cessation of growth (while other stalagmites continued their growth) may be explained by frost-related mass movements on the surface and/or clogging of specific percolation flow-paths within the rock mass causing water to emerge at other stalactites nearby. Another possibility would be corrosional exposure of sulphide grains in the mica schist/marble interface which, upon oxidation, would release sulphuric acid and suppress supersaturation. The sample was selected for its length and hence temporal resolution, and this somewhat unfortunate fact was only detected after the sample was split open and dated.

Climatic conditions during LIA are quite well known in Norway. Based on the depression of equilibrium-line altitude (ELA) of glaciers that expanded during the LIA maximum (~150 m), combined with the adiabatic lapse rate of 0.6°C/100 m (Green and Harding, 1980), this corresponds to a drop in *mean summer temperature* of about ~1°C relative to the present (Nesje and Kvamme, 1991), provided that precipitation was similar in the two cases. This estimate was done for glaciers in southwestern Norway, but there is little reason to believe that the magnitude of this temperature shift was radically different in northern Norway. This assumption is further supported by recent studies of Greenland ice cores (Fischer *et al.*, 1998), which suggest a temperature drop during LIA of at least 1°C relative to the present. Assuming that the cave temperature drop during LIA responded similarly to the drop in mean summer temperature at the surface, the present-day LIA temperature difference is taken as a first approximation for calibrating the SDF for sample SG93, Table 3. Combining equations (1) and (3) with the $\Delta\delta^{18}O_c/\Delta T$ of –0.32‰ °C^{-1} (calculated from LIA and present-day $\delta^{18}O_c$, *vide infra*), yields c

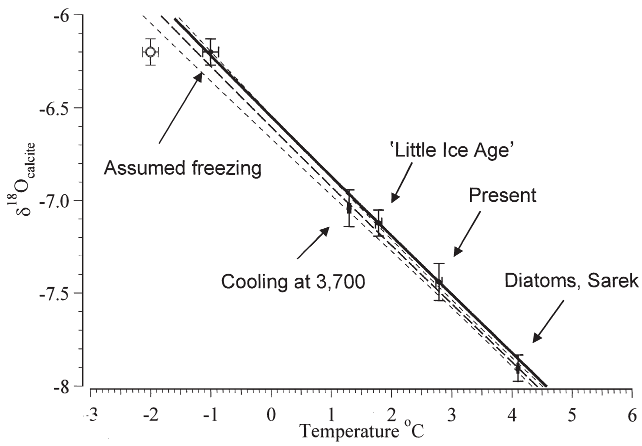

Figure 8 Calibration of the Speleothem Delta Function (SDF), using data from Table 3. Thick line: regression of SDF based on two input values, the present-day conditions, and the 'Little Ice Age' (LIA) temperature drop. Extrapolation of this line fits quite well with the other temperature estimates (they have negligible $\Delta_{SMOW}(t)$ corrections). One exception is the temperature for 'assumed freezing', corrected for Δ_{SMOW} at 10 000 cal BP (–2°C, open circle with error bars), whilst the uncorrected temperature estimate (–1°C) fits quite well The dashed line with confidence intervals shows regression of SDF based on all five data points, using the uncorrected temperature for 'assumed freezing'.

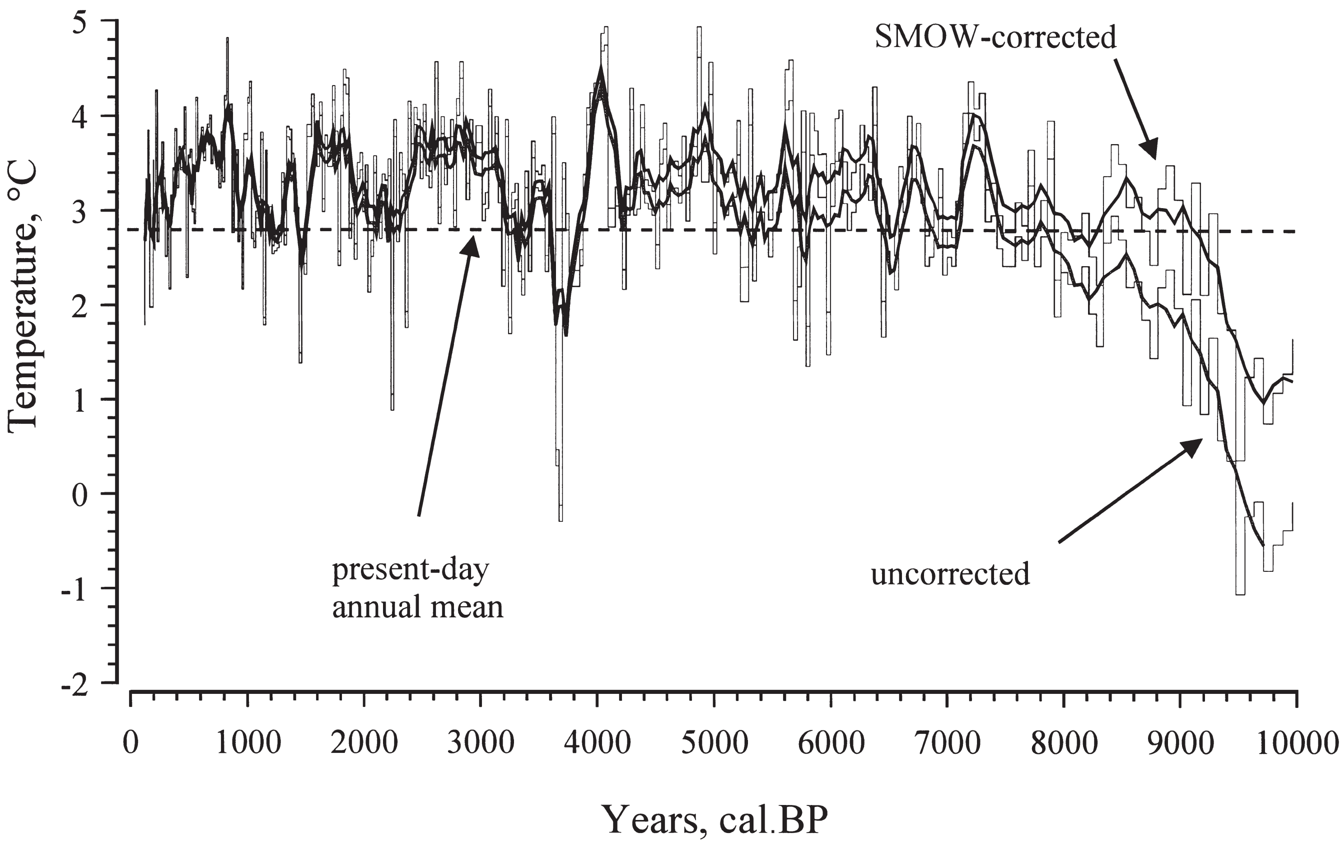

Figure 9 The effect of Δ_{SMOW} correction on the temperature time-series of SG93: lower curve, temperatures calculated from the calibrated SDF without $\Delta_{SMOW}(t)$ correction; upper curve, the calculation done with $\Delta_{SMOW}(t)$ correction. Thin lines represent primary data; thick lines five-point running mean.

= –0.053 and d = –9.54. No errors can be associated with these two parameters, as the degree of freedom is 0. Using these constants, the SDF plots as the thick solid line in Figure 8.

Testing against other possible calibration points

We may now test if other independent temperature estimates (Table 3) are in agreement with the calibrated SDF when it is extrapolated beyond the present day-LIA temperature interval. This is done in Figure 8 by first plotting the other temperature estimates (Table 3) together with the LIA-calibrated SDF, and then including them in the regression. These points are all corrected for $\Delta_{SMOW}(t)$, although this correction is only significant for t > about 7000 cal. BP (Table 3).

When extrapolated beyond its calibration range, the LIA-calibrated SDF (thick line, Figure 8) also predicts the other data points quite well. However, for the oldest point, commencement of speleothem growth after permafrost conditions, the $\Delta_{SMOW}(t)$-correction shifts this calibration point away from the extrapolated SDF line, while the uncorrected data point does fit quite well. This suggests either that the basal layer in the speleothem does not represent the immediate post-permafrost temperature or that the assumption of time-invariance for the dripwater function breaks down at this time.

The internal error in $\delta^{18}O_c$ measurements is ±0.7‰ vPDB, and the error in the temperature estimates were set to ±0.2°C. Regression then yields estimates of the constants equation (5):

$$c = -0.0429 \pm 0.0083$$

$$d = -15.48 \pm 0.29$$

i.e., with relative errors of *c.* 1.9%. However, when substituted into the speleothem delta function and solved for T, this converts to a systematic error in temperature of 1.79°C, of which 0.16°C is due to the internal error in the $\delta^{18}O_c$ measurements. The absolute precision in temperature estimates is thus ±1.8°C, of which changes between data points greater than ±0.16°C are significant. The precision in this transfer function is dependent on the number and precision of the data points that goes into the regression, and may be improved when more calibration data become available.

These parameters can now be substituted into the SDF and solved for T using the Newton-Rapson method. The result is shown for the whole time-series as the lower curve in Figure 9. The $\Delta_{SMOW}(t)$ term can now be introduced and the temperatures recalculated. The effect of the $\Delta_{SMOW}(t)$-correction is a positive temperature shift for the older part of the curve of up to 1.2°C around 10 000 cal. BP.

Testing the temperature calibration against other temperature records

In the absence of measured temperatures, the only way to test the correctness of any transfer function is to test the results against another well-established proxy. In this case we have used two tests: the GISP2 ice core and the historic record. The tests are reviewed briefly below. The temperature record is discussed in greater detail in a companion paper to this one.

GISP2 ice-core record

The temperature curves for the last 10 kyrs of GISP2 and SG93 presented in Figure 10 may be summarized as follows.

- A comparison of the curves reveals a general correlation in timing, duration, and direction although perhaps not in magnitude of events for the majority of the record.
- In addition to the obviously lower temperatures, GISP2 shows a greater range of temperature changes than SG93 (1°C change in SG93 corresponds to around 1.6°C in GISP2).
- The correlation between the two curves is weakest for the first very slow 1000 years of SG93's growth.

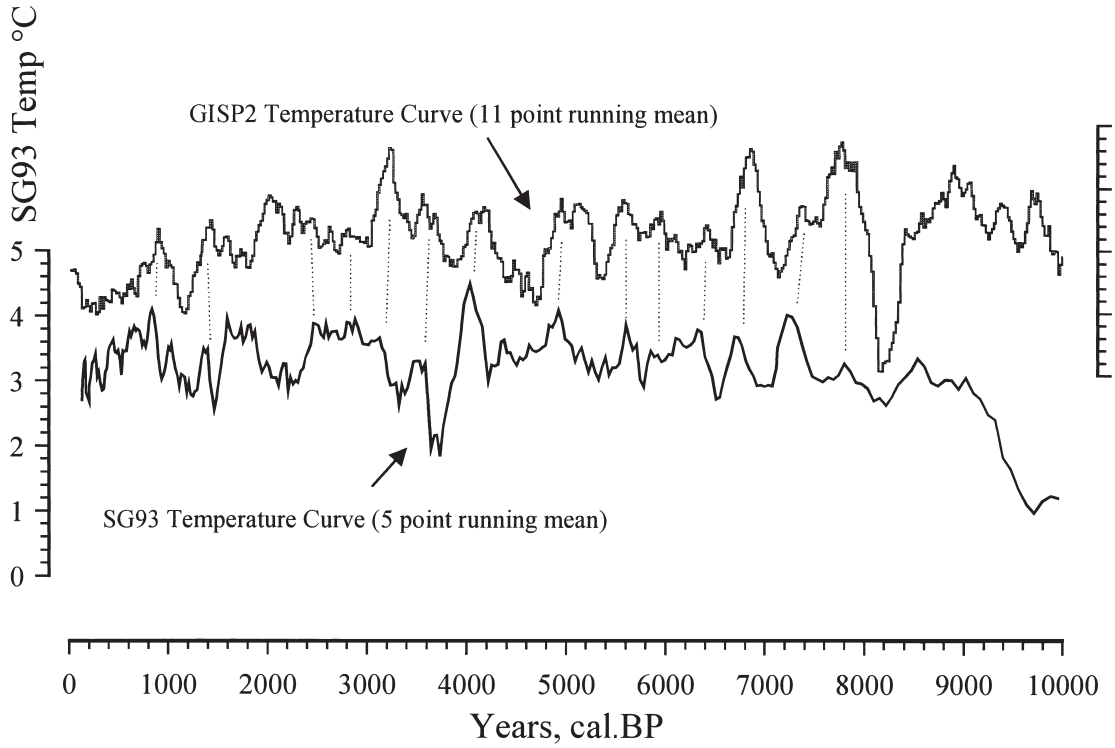

Figure 10 Temperature curves for the last 10 kyrs: GISP2 (upper curve) and SG93 (lower curve). Some of the coincident peaks are indicated with dotted lines.

- Between 8000 and 4000 cal. BP the correlation is remarkably high.
- While the directions of changes are similar, SG93 shows greater variations between 4000 and 3500 cal. BP.
- The correlation is not so clear from 3500 to 2500 cal. BP and breaks down at 2500 cal. BP. However it is of interest that GISP2 does not correlate with the other Greenland Summit ice core, GRIP, at this point.
- SG93 correlates better with the historic record (*vide infra*) than it does with GISP2 for the period 2000–1000 cal. BP. The higher temperatures of the Roman Empire times are apparent only in SG93.
- The correlation is again remarkable for the last 1000 years down to the 'Little Ice Age' when SG93 stopped growing.

Historic record

Although dates of climatic events in the historic records are legion, estimates of the magnitude of events are scarce. Most of the quantitative information available is only for the 'Little Ice Age', which has already been used for the calibration and thus cannot be used for the test. The historic record is therefore more of a test of the dating than of the absolute temperature reconstruction. However, the sense of events can be clearly compared.

Most of the information for historical climate changes has been gleaned from Crowley and North (1991). The SG93 record for the last two millennia has been plotted in Figure 11 together with some of these important historic events.

- The Roman Empire, established in 27 BC (Thompson, 1993) coincided with a period of warmer temperatures indicated in SG93 as at least 1°C above the modern mean. The decline (after the division in AD 395) followed closely the climatic deterioration which began in the SG93 record at around AD 400.
- The Dark Age (Medieval) Cold Epoch is estimated at AD 500–1000 and is clearly shown in the SG93 record.
- The Medieval Optimum is estimated at ~ AD 1100–1300, matched closely by the SG93 record. Temperature estimates from central England temperatures show a peak of ~1–1.5°C above the mean, centred on AD 1200, which matches the similar peak in SG93 centred on AD 1160.
- Summer temperatures in Paris for the period AD 1350–1850 were reconstructed from grape harvest data (Crowley and North, 1991). It is of interest that, except for the nineteenth century, the 'Little Ice Age' cooling is not greatly manifest in the summer temperatures and that the SG93 record agrees rather well with them. This is not surprising since a speleothem in a region of winter frozen ground is likely to show a bias towards summer precipitation. The warm periods with peaks in AD 1375 and 1425 of ~0.9°C above the mean and another around AD 1650–1700 are matched in the SG93 record.

The beginning of climatic deterioration to the 'Little Ice Age' started at around AD 1450 (Crowley and North, 1991). The cold phase had two troughs of about a century's duration, in the seventeenth and nineteenth centuries, with the coldest decades in the mid- to late 1600s, early 1800s and late 1800s. Each of these three troughs is matched in SG93. (It is of interest to note that the Paris summer temperatures show a peak of ~0.9°C *above* mean around AD 1650–1700 which is in the middle of the supposed coldest decades). The average temperature range of LIA in SG93 would appear rather high but agrees with the temperatures from central England which only go marginally below the mean from AD 1550 to 1700.

Conclusions

The close correlation of the SG93 temperature record with the GISP2 ice-core record and the historic record suggests: (1) that the technique of temperature reconstruction using the speleothem delta function is valid; and (2) that the temperatures in this northern Norwegian cave located relatively close to the coast do indeed reflect global or at least hemispherical trends. We conclude that the speleothem delta function is a reliable and promising tool for deriving absolute temperatures from speleothems. These principles can be applied in any region but the details of calibration

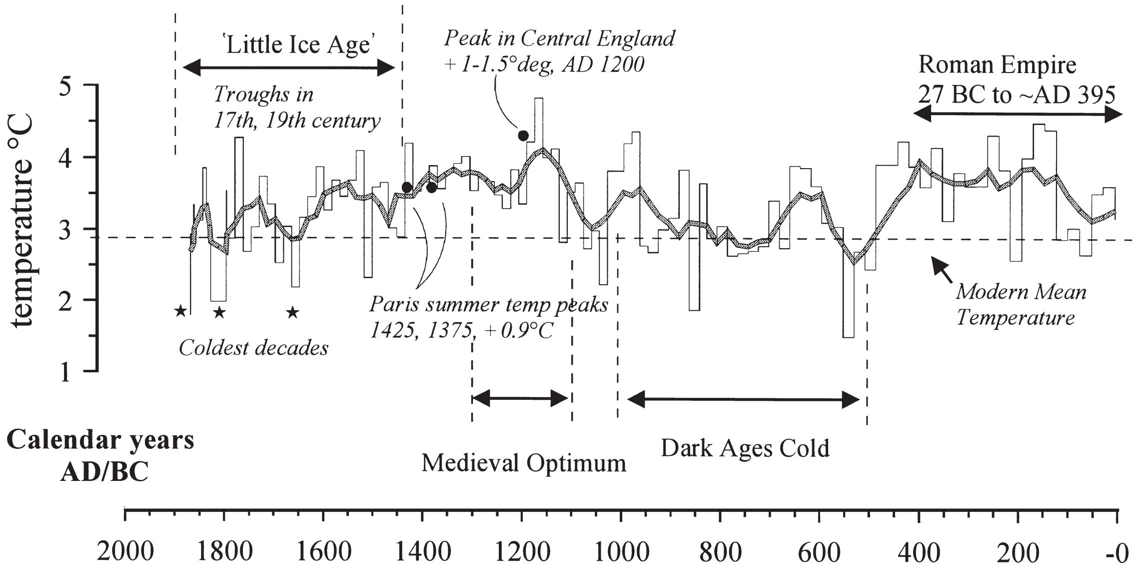

Figure 11 The speleothem temperature history inferred for the last 2000 years compared with known 'historic' events.

of the function must be specific for each region and each speleothem studied.

Acknowledgements

Financial support was provided by NFR grant 122226/720. U-series dates were done at the Uranium Series Dating Laboratory at the Department of Geology, University of Bergen. The Royal Ministry of Environment and 'Statens Skoger' provided permission to sample the speleothems. The Sandhei family is thanked for their hospitality and help during fieldwork in the years 1991–1998. Data for GISP2 ice core were provided by the National Snow and Ice Data Center, University of Colorado at Boulder, and the WDC-A for Paleoclimatology, National Geophysical Data Center, Boulder, Colorado.

References

Alley, R.B., Mayewski, P.A., Sowers, T., Stuiver, M., Taylor, K.C. and **Clark, P.U.** 1997: Holocene climatic instability: a prominent, widespread event 8200 yr ago. *Geology* 25, 483–86.

Baker, A., Smart, P.L., Edwards, R.L. and **Richards, D.A.** 1993: Annual growth banding in a cave stalagmite. *Nature* 364, 518–20.

Barnekow, L. and **Berglund, B.E.** 1998: Holocene vegetation and climate changes in the Abisko area – studies of pollen and macrofossils in lake sediments. *Abstract volume of the CIRC Climate Workshop, Abisko, 5–7 October*.

Bastin, B. 1978: L'analyse pollinique des stalagmites: une nouvelle possibilité d'approche des fluctuations climatiques du quaternaire. *Annales de la Societé Geologique de Belgue* 101, 13–19.

Chen, J.H., Edwards, R.L. and **Wasserburg, G.J.** 1992: Mass spectrometry and application to uranium-series disequilibrium. In Ivanovich, M. and Harmon, R.S., editors, *Uranium-series disequilibrium: applications to earth, marine, and environmental sciences*, Oxford: Clarendon Press, 174–206.

Craig, H. 1961: Isotopic variation in meteoric waters. *Science* 133, 1702–703.

Crowley, T.J. and **North, G.R.** 1991: *Paleoclimatology*. New York: Oxford University Press, 339 pp.

Dansgaard, W. 1964: Stable isotopes in precipitation. *Tellus* 16, 436–68.

DNMI 1998: *Temperature data for Neveenes meteorological station, Mo i Rana*. Oslo: Det Norske Meteorologiske Institutt.

Dorale, J.A., Gonzàles, L.A., Reagan, M.K., Pickett, D.A., Murrell, M.T. and **Baker, R.G.** 1992: A high-resolution record of Holocene climate change in speleothem calcite from Cold Water Cave, northeast Iowa. *Science* 258, 1626–30.

Einevoll, S. and **Lauritzen, S.E.** 1994: Calibration of stable isotope and temperature signal in the percolation zone of a sub-arctic cave, northern Norway. *Cave and Karst Science* 21, 9.

Fischer, H., Werner, M., Wagenbach, D., Schwager, M., Thorsteinnson, T., Wilhelms, F. and **Kipfstuhl, J.** 1998: 'Little Ice Age' clearly recorded in northern Greenland ice cores. *Geophysical Research Letters* 25, 1749–52.

French, H.M. 1976: *The periglacial environment*. New York: Longman, 309 pp.

Friedman, I. and **O'Neil, J.R.** 1977: Compilation of stable isotope fractionation factors of geochemical interest. *US Geological Survey Professional Paper P-0440-KK*, 1–12.

Fritz, P. and **Fontes, J.C.** 1980: Introduction. In Fritz, P. and Fontes, J.C., editors, *Handbook of evironmental isotope geochemistry*, Amsterdam: Elsevier, 1–20.

Gascoyne, M. 1992: Palaeoclimate determination from cave calcite deposits. *Quaternary Science Reviews* 11, 609–32.

Gat, J.R. 1980: The isotopes of hydrogen and oxygen in precipitation. In Fritz, P. and Fontes, J.C., editors, *Handbook of evironmental isotope geochemistry*, Amsterdam: Elsevier, 21–48.

Green, F.H.W. and **Harding, R.J.** 1980: The altitudinal gradients of air temperature in southern Norway. *Geografiska Annaler* 62A, 29–36.

Hall, R.I., Rosen, P., Renberg, I. and **Segerstrøm, U.** 1998: Holocene climate change: paleolimnological data fraom the Sarek mountains. *Abstract volume of the CIRC Climate Workshop, Abisko, 5–7 October*.

Hendy, C.H. 1971: The isotopic geochemistry of speleothems. Part 1. The calculation of the effects of different modes of formation on the isotopic composition of speleothems and their applicability as paleoclimatic indicators. *Geochimica Cosmochimica Acta* 35, 801–24.

Latham, A.G. and **Schwarcz, H.P.** 1992: Carbonate and sulphate precipitates. In Ivanovich, M. and Harmon, R.S., editors, *Uranium-series disequilibrium: applications to Earth, marine, and environmental sciences*, Oxford: Clarendon Press, 423–59.

Lauritzen, S.E. 1995: High-resolution paleotemperature proxy record during the last interglaciation in Norway from speleothems. *Quaternary Research* 43, 133–46.

— 1996: Calibration of speleothem stable isotopes against historical records: a Holocene temperature curve for north Norway? *Karst Waters Institute Special Publication* 2, 78–80.

Lauritzen, S.E. and **Lundberg, J.** 1997a: DIXIELAND: a program for outlier analysis on raw count data of Th and U from Finnigan MAT 262 RPQ. Turbo Pascal Code. Department of Geology, Bergen University.

— 1997b: TIMS Age4U2U: a program for raw data processing, error

propagation and $^{230}Th/^{234}U$ age calculation for mass spectrometry. Turbo Pascal Code. Department of Geology, Bergen University.
— 1998: Rapid temperature variations and volcanic events during the Holocene from a Norwegian speleothem record. *Proceedings of the PAGES Open Science Meeting, University of London, 20–23 April 20–23*, 88.
Lauritzen, S.E., Ford, D.C. and **Schwarcz, H.P.** 1986: Humic substances in speleothem matrix – paleoclimatic significance. *Proceedings, 9th International Speleological Congress. Barcelona* 1, 77–79.
Lauritzen, S.E., Løvlie, R., Moe, D. and **Østbye, E.** 1990: Paleoclimate deduced from a multidiciplinary study of a half-million year-old stalagmite from Rana, northern Norway. *Quaternary Research* 34, 306–16.
Martinson, D.G., Pisias, N.G., Hays, J.D., Imbrie, J., Moore, T.C. and **Shackleton, N.J.** 1987: Age dating and the orbital theory of the ice ages: development of a high-resolution 0 to 300000 yr chronostratigraphy. *Quaternary Research* 27, 1–29.
Nesje, A. and **Kvamme, M.** 1991: Holocene glacier and climate variations in western Norway: evidence for early Holocene glacier demise and multiple Neoglacial events. *Geology* 19, 610–12.
O'Neil, J.R., Clayton, R.N. and **Mayeda, T.** 1969: Oxygen isotope fractionation in divalent metal carbonates. *Journal of Chemical Physics* 51, 5547–58.
Price, L.W. 1972: *The periglacial environment, permafrost, and man*. Washington DC: Association of American Geographers, 88 pp.
Ramseyer, K., Miano, T., D'Orazio, V., Wildberger, A., Wagner, T. and **Geister, J.** 1997: Nature and origin of organic matter in carbonates from speleothems, marine cements and coral skeletons. *Organic Geochemistry* 26, 361–78.
Rowe, P.J., Dennis, P.F., Atkinson, T.C., Lauritzen, S.E. and **Lundberg, J.** 1998: A high resolution deuterium record from fluid inclusions in a late Holocene speleothem from S.W. Britain. *Proceedings of the PAGES Open Science Meeting, University of London, 20–23 April*, 112.
Schwarcz, H.P. 1980: Absolute age determinations of archaeological sites by uranium dating of travertines. *Archaeometry* 22, 3–24.
— 1986: Geochronology and isotope geochemistry in speleothems. In Fritz, P. and Fontes, J., editors, *Handbook of environmental isotope geochemistry*, Amsterdam: Elsevier, 271–303.
Schwarcz, H.P. and **Yonge, C.** 1983: Isotopic composition of paleowaters as inferred from speleothem and its fluid inclusions. In Gonfiantini, R., editor, *Paleoclimates and paleowaters; a collection of environmental isotope studies*. Vienna: International Atomic Energy Agency, Vienna, Austria.
Shackleton, N.J. and **Opdyke, N.D.** 1973: Oxygen isotope and palaeomagnetic stratigraphy of equtorial Pacific core V-28–238: oxygen isotope temperatures and ice volumes on a 10^5 year and 10^6 year scale. *Quaternary Research* 3, 39–55.
Shopov, Y., Ford, D.C. and **Schwarcz, H.P.** 1994: Luminescent microbanding in speleothems: high-resolution chronology and paleoclimate. *Geology* 22, 407–10.
Talma, A.S. and **Vogel, J.C.** 1992: Late Quaternary paleotemperatures derived from a speleothem from Cango Caves, Cape Province, South Africa. *Quaternary Research* 37, 203–13.
Thompson, D. 1993: *The Oxford dictionary of current english*. Oxford: Oxford University Press, 1074 pp.
Wigley, T.M.L. and **Brown, M.C.** 1976: The physics of caves. In Ford, T.D. and Cullingford, C.H.D., editors, *The science of speleology*, London: Academic Press, 329–58.